



# L'ANTIFERROMAGNÉTISME

— 1936 —



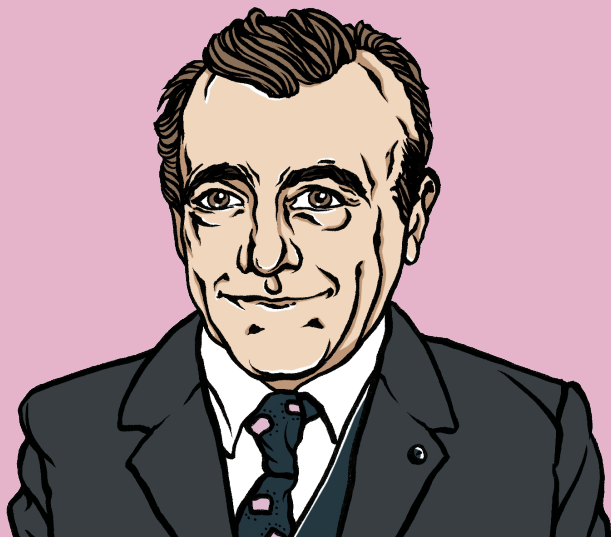
# L'ANTIFERROMAGNÉTISME



INSTITUT DE PHYSIQUE DE STRASBOURG, FRANCE



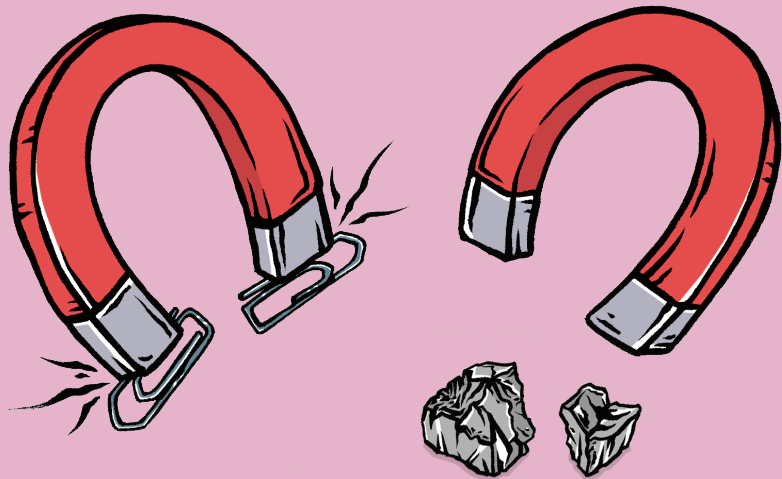
# L'ANTIFERROMAGNÉTISME



L. NÉEL



# L'ANTIFERROMAGNÉTISME



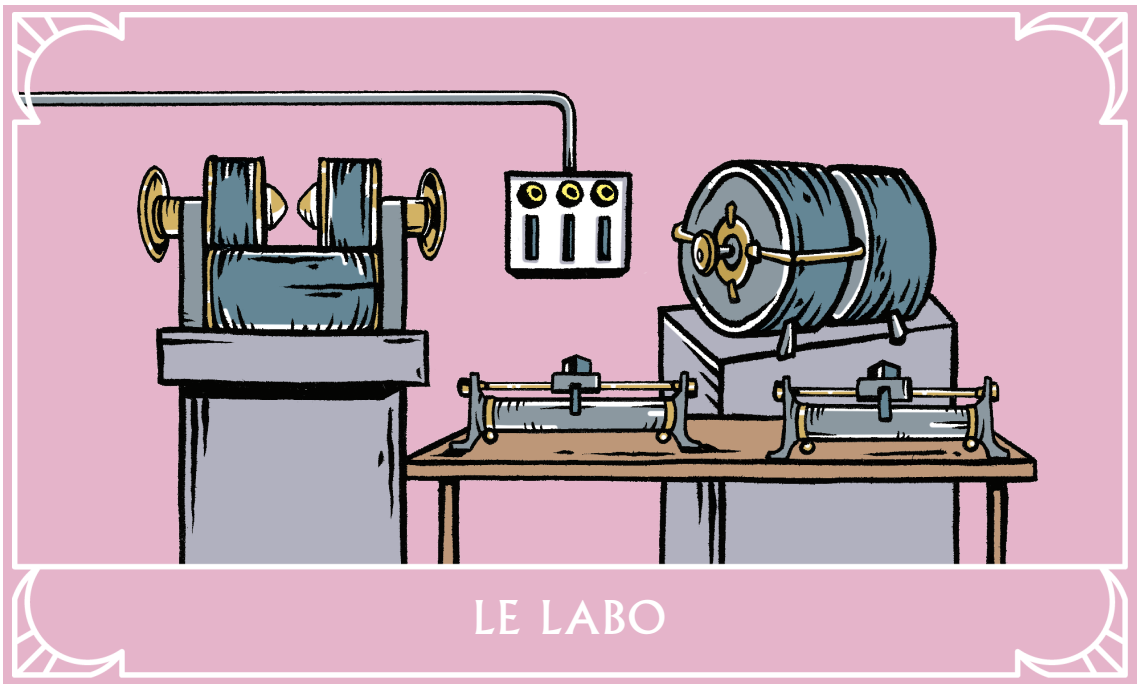
## LA QUESTION

Pourquoi certains métaux ou oxydes, par exemple le chrome, ne semblent pas magnétiques ?



# L'ANTIFERROMAGNÉTISME

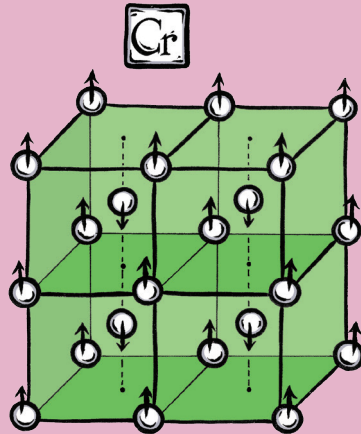
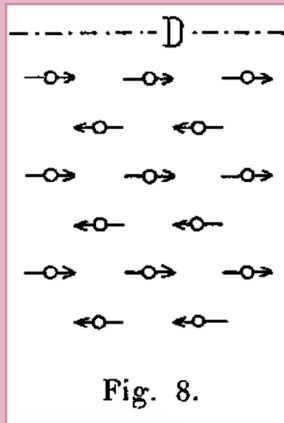




LE LABO



# L'ANTIFERROMAGNÉTISME



## LE RÉSULTAT

Dans certains métaux et oxydes, les atomes portent de petits aimants, les spins, qui s'organisent tête-bêche. Ces matériaux appelés antiferromagnétiques ne présentent plus de pôles même si ils sont aussi ordonnés qu'un vrai aimant.



# L'ANTIFERROMAGNÉTISME

PROPRIÉTÉS MAGNÉTIQUES  
DE L'ÉTAT MÉTALLIQUE ET ÉNERGIE  
D'INTERACTION ENTRE ATOMES  
MAGNÉTIQUES

Par M. LOUIS NÉEL

SOMMAIRE. — Une première partie du travail (§ 1 à 10) est consacrée à l'interprétation des expériences de M. Manders sur les variations, en fonction de la température, de la susceptibilité magnétique de quelques solutions solides à base de nickel (Ni et Al) ou de Ti, Sn, Sb, V, Mo, W, Cr). On étudie et on interprète les variations, en fonction du titre, de la constante de Curie et du coefficient de paramagnétisme constant superposé. On en déduit que les électrons magnétiques du nickel restent en nombre constant lorsqu'on passe de l'état ferro à l'état paramagnétique.

Dans une deuxième partie (§ 11 à 29), on expose comment on peut définir et calculer une énergie d'interaction magnétique entre deux atomes voisins porteurs de moment, à partir des données expérimentales, soit pour les ferromagnétiques, soit pour les corps à champ moléculaire négatif (Pd et Pt), soit pour les corps paramagnétiques à susceptibilité indépendante de la température (Mn, Cr, Ti, Mo, Ru, Rh, etc.). On étudie ensuite les variations de l'énergie d'interaction avec la distance entre les couches magnétiques des atomes interagissant et on montre qu'en première approximation l'énergie d'interaction ne dépend que de cette distance et varie très régulièrement avec elle. Cette conception permet d'interpréter et de relier entre eux un certain nombre de faits expérimentaux dont quelques-uns sont passés en revue.

Enfin, en supposant qu'il existe un couplage entre le réseau cristallin et les spins responsables du magnétisme des métaux, apparaissent des propriétés curieuses qui semblent être un point de départ pour expliquer les propriétés magnétiques compliquées du platine (§ 18, 19 et 20).

§ 16. Calcul de  $\omega_{AB}$  d'après les données expérimentales. — Si la concentration du métal B est petite, on a :

$$V = P\alpha'_A + Q \frac{\mu_B}{\mu_A} C_B \quad \text{et} \quad C' = PC_A + QC_B \left( \frac{\mu_B}{\mu_A} - \frac{\theta'}{\theta} \right) \quad (11)$$

soit, en fonction du titre, une variation linéaire du point de Curie et de la constante de Curie apparente. Prolongeons les droites obtenues jusqu'à  $Q = 1$  ; soit  $\theta'$  et  $C'$  les valeurs de  $\theta$  et  $C'$  correspondant à  $Q = 1$ , d'après (11) on a :

$$\frac{C'}{\theta'} = \frac{P}{\theta} - \frac{1}{\alpha} \quad \text{ou} \quad b = \frac{3}{\frac{P}{\theta} + \frac{1}{\alpha}} \quad (12)$$

en remarquant que pour le métal A pur, de constante de Curie  $C_A$  et de point de Curie  $\theta_A$ , on a :  $a = \frac{\theta_A}{C_A}$ .  $C'$  et  $\theta'$  se déterminent expérimentalement en extrapolant les tangentes initiales aux courbes de variation de la constante de Curie et du point de Curie en fonction du titre. J'ai appliqué cette méthode pour calculer les énergies d'interaction des liaisons mixtes  $\omega_{AB}$  : Ni-Co, Ni-Fe, Co-Fe, d'après les données expérimentales de Preuss (10), de Foschard (11) et de Bloch (14).

Dans le calcul précédent,  $\omega_{AB}$  représente l'énergie totale d'interaction entre deux moments  $\mu_A$  et  $\mu_B$ . Pour avoir des valeurs comparables aux  $\omega$  du § 14, il faut exprimer  $\omega_{AB}$  au moyen de l'énergie  $\omega_{AB}$  d'interaction de deux électrons, portés l'un par l'atome A et l'autre par l'atome B. Posons  $\mu_A = g\mu_B$ ,  $\mu_B = g'\mu_B$  en désignant par  $\mu_B$  le magnéton de Bohr. On a immédiatement :  $\omega_{AB} = gg'\omega_{AB}$ . D'où, d'après la formule 8, puisque le facteur  $gg'$  disparaît haut et bas :

$$b = \frac{3\omega_{AB}}{8\mu_B^2} \quad (13)$$

Le tableau 5 donne les valeurs de  $C'$ ,  $\theta'$ ,  $\omega_{AB}$  correspondant à différentes liaisons. Le système cristallin étant le cube à faces centrées, on a toujours :  $2\mu = 12$ .

région où la formule 3 n'est pas valable, d'où la nécessité d'une étude spéciale de cette région qui sera pour les corps



Fig. 8.

à champ moléculaire négatif la réplique de la région ferromagnétique des corps à champ moléculaire positif.

Au zéro absolu, chaque atome se dispose antiparallèlement à ses voisins, de manière à réaliser un assemblage d'énergie



Fig. 9.

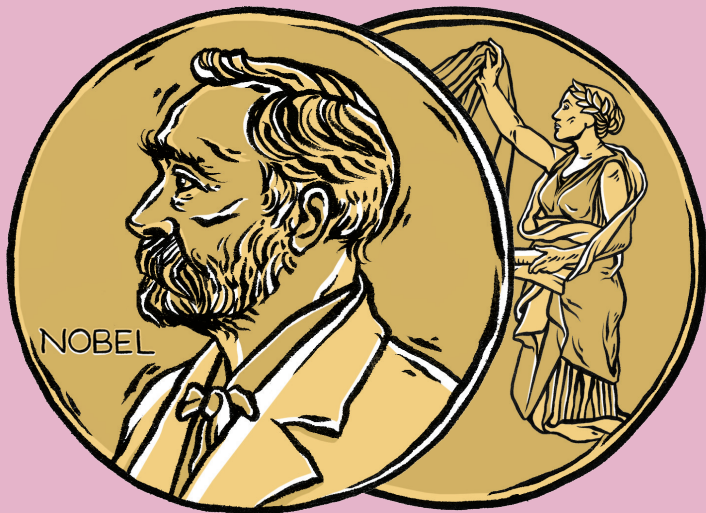
potentielle minimum comme celui qui est représenté sur la figure 8. Les moments sont tous parallèles à une même direction D, mais ils sont dirigés dans des sens différents au lieu d'être tous de même sens comme dans les ferromagnétiques. Un champ magnétique  $H$ , perpendiculaire à la direction D, va déformer cet assemblage et l'aîmester. Tous les

# L'ARTICLE

Propriétés magnétiques de l'état métallique et énergie d'interaction  
entre atomes magnétiques, L. Néel, Annales de Physique, 5, 232 (1936)



# L'ANTIFERROMAGNÉTISME



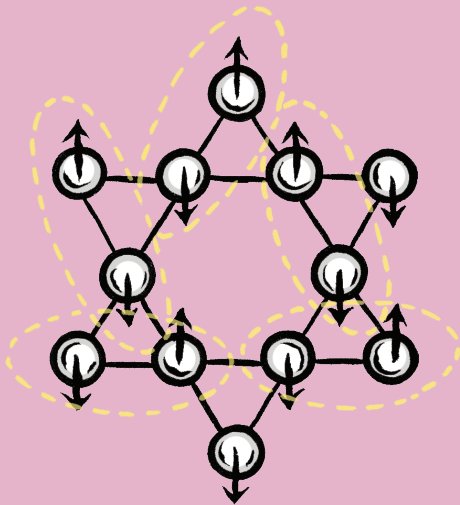
## L. NÉEL, PRIX NOBEL, 1970

Pour la découverte de l'antiferromagnétisme et du ferrimagnétisme qui ont mené à d'importantes applications en physique des solides.



# L'ANTIFERROMAGNÉTISME





## AUJOURD'HUI

De nouvelles formes d'aimants sont au cœur des recherches actuelles. Par exemple, dans les « liquides de spin », les spins placés en étoiles refusent de s'ordonner et se placent dans plusieurs états quantiques à la fois.



# L'ANTIFERROMAGNÉTISME



# LE GRAPHÈNE

— 2004 —



# LE GRAPHÈNE



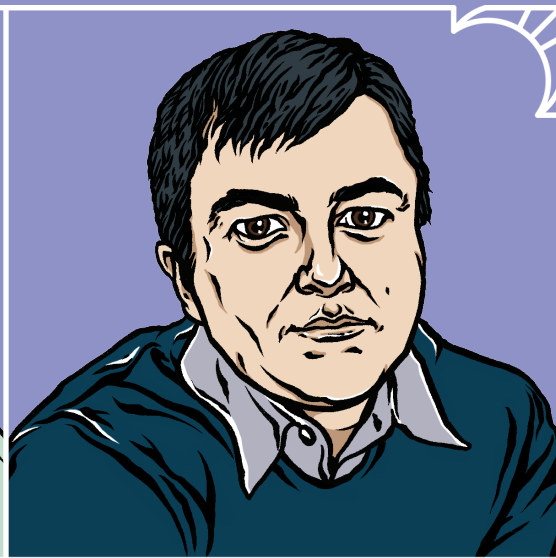
UNIVERSITÉ DE MANCHESTER, ANGLETERRE



# LE GRAPHÈNE



A. GEIM

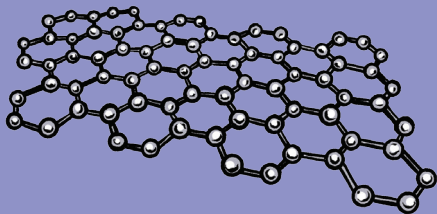
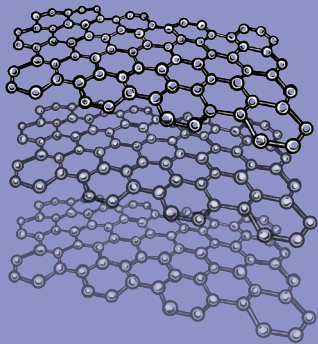


K. NOVOSELOV



# LE GRAPHÈNE



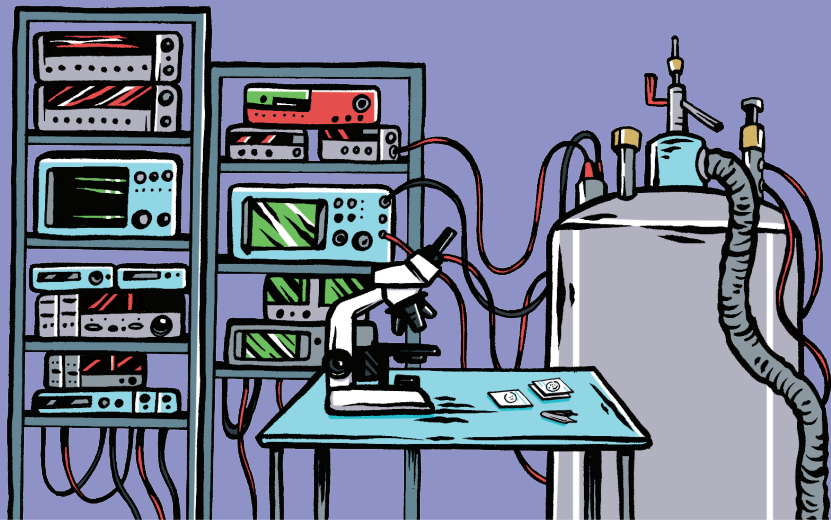


## LA QUESTION

Peut-on fabriquer une couche d'un seul atome d'épaisseur à partir du charbon ?  
Et quelles seraient alors ses propriétés ?



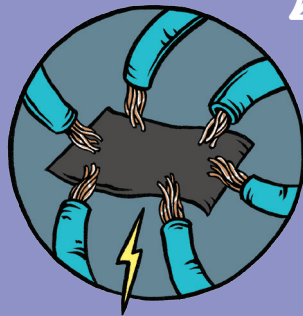
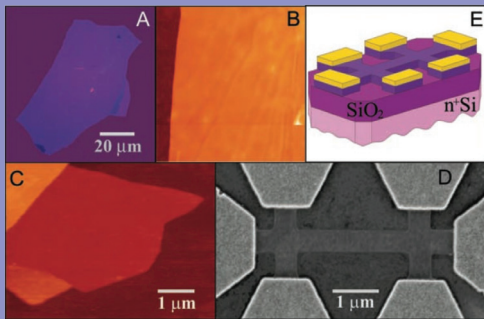
# LE GRAPHÈNE



LE LABO



# LE GRAPHÈNE



## LE RÉSULTAT

On peut fabriquer, observer et mesurer une seule couche d'atomes de carbone, appelée graphène. Elle présente des propriétés électriques étonnantes, ni tout à fait métalliques, ni tout à fait isolantes.



# LE GRAPHÈNE

**REPORTS**

**Fig. 1. Conductance modulation (CM) to show the field-effect on the spin direction of the signal channel is used in the peak of electron temperature for  $\sim 100$  mK above room temperature and the values of the area under each crossing transition are arbitrary.**

Area	100 K	100 K	100 K	100 K
$\sigma_{11}$	0.78 ± 0.02	0.82 ± 0.02	0.88 ± 0.02	0.79 ± 0.02
$\sigma_{22}$	0.71 ± 0.02	0.65 ± 0.02	0.60 ± 0.02	0.71 ± 0.02



**Fig. 2. Time-dependent magnetotransport stability of the signal and the field-effect for  $\sim 100$  mK above room temperature.**

Arbitrary offsets for the read lines are 0.1 units. The error bars are standard deviations of the data points from the fit.

We have realized a quantum state by controlling the magnetotransport of atomic spin.

**Electric Field Effect in Atomically Thin Carbon Films**

K. S. Novoselov,<sup>1</sup> A. K. Geim,<sup>1</sup> S. V. Morozov,<sup>2</sup> D. Jiang,<sup>1</sup> Y. Zhang,<sup>1</sup> S. V. Dubonos,<sup>1</sup> I. V. Grigorieva,<sup>1</sup> A. A. Firsiroti<sup>1</sup>

We describe nonmetallic graphitic films, which are a new two-dimensional quantum state of carbon. They are ultrathin and stable under ambient conditions, and of remarkably high quality. The films are based on the novel two-dimensional material graphene, which consists of a single atomic layer of carbon atoms with sp<sup>2</sup> hybridized orbitals forming a honeycomb lattice. The carrier concentration can be tuned by applying a gate voltage.

The ability to control electronic properties of a material by externally applied fields is at the heart of modern electronics. In semiconductors, it is the electric field effect that allows us to vary the carrier concentration in a controlled device and, consequently, change an electric current through it. In the case of metals, the carrier concentration is determined by the density of states at the Fermi level, which is not tunable by an external field. In this work, we report on the realization of a new material that is stable under ambient conditions and can be tuned by an external field. It is a single layer of carbon atoms, which we call graphene. It is a two-dimensional material, which is stable under ambient conditions and can be tuned by an external field. It is a single layer of carbon atoms, which we call graphene. It is a two-dimensional material, which is stable under ambient conditions and can be tuned by an external field.

Two-dimensional carbon nanotubes (1D), nanoribbons (2D), and nanosheets (2D) are the most likely. Because the carrier field is a natural property of the material, it can be used to tune the carrier concentration in a controlled device and, consequently, change an electric current through it. In the case of metals, the carrier concentration is determined by the density of states at the Fermi level, which is not tunable by an external field. In this work, we report on the realization of a new material that is stable under ambient conditions and can be tuned by an external field. It is a single layer of carbon atoms, which we call graphene. It is a two-dimensional material, which is stable under ambient conditions and can be tuned by an external field.

nonmetallic material is using the field-effect transistor (FET). Graphene is a naturally occurring material, which is stable under ambient conditions. It is a single layer of carbon atoms, which we call graphene. It is a two-dimensional material, which is stable under ambient conditions and can be tuned by an external field. It is a single layer of carbon atoms, which we call graphene. It is a two-dimensional material, which is stable under ambient conditions and can be tuned by an external field.

We have been able to prepare graphene sheets of thickness down to a few atomic layers (thickness range from 1 to 10 layers) by the chemical exfoliation of graphite. The carrier concentration in the sheets can be tuned by the chemical doping of the sheets with various molecules. The carrier concentration in the sheets can be tuned by the chemical doping of the sheets with various molecules. The carrier concentration in the sheets can be tuned by the chemical doping of the sheets with various molecules.

The carrier concentration in the sheets can be tuned by the chemical doping of the sheets with various molecules. The carrier concentration in the sheets can be tuned by the chemical doping of the sheets with various molecules. The carrier concentration in the sheets can be tuned by the chemical doping of the sheets with various molecules. The carrier concentration in the sheets can be tuned by the chemical doping of the sheets with various molecules.

The carrier concentration in the sheets can be tuned by the chemical doping of the sheets with various molecules. The carrier concentration in the sheets can be tuned by the chemical doping of the sheets with various molecules. The carrier concentration in the sheets can be tuned by the chemical doping of the sheets with various molecules. The carrier concentration in the sheets can be tuned by the chemical doping of the sheets with various molecules.

The carrier concentration in the sheets can be tuned by the chemical doping of the sheets with various molecules. The carrier concentration in the sheets can be tuned by the chemical doping of the sheets with various molecules. The carrier concentration in the sheets can be tuned by the chemical doping of the sheets with various molecules. The carrier concentration in the sheets can be tuned by the chemical doping of the sheets with various molecules.

graphene ( $\sim 100$  nm), the carrier mobility is  $1.5 \times 10^4$  cm<sup>2</sup>/Vs. The electric field doping technique allows carrier concentration to be varied over a range of  $10^4$  cm<sup>-3</sup> to  $10^{18}$  cm<sup>-3</sup>. The carrier concentration in the sheets can be tuned by the chemical doping of the sheets with various molecules. The carrier concentration in the sheets can be tuned by the chemical doping of the sheets with various molecules.

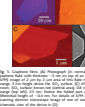


**Fig. 2. Scanning electron micrographs (SEM) of individual graphene sheets. (a) A large, flat, rectangular sheet. (b) A smaller, more irregular sheet. (c) A sheet with a distinct edge. (d) A sheet with a distinct edge and a small hole.**



**Fig. 3. Raman spectra showing the intensity of the G and 2D bands as a function of the magnetic field.**

**REPORTS**

electron in hole. In  $R_{xx}$  devices with increasing carrier concentration in the read line. The carrier concentration in the read line can be tuned by the chemical doping of the sheets with various molecules. The carrier concentration in the read line can be tuned by the chemical doping of the sheets with various molecules.

The carrier concentration in the read line can be tuned by the chemical doping of the sheets with various molecules. The carrier concentration in the read line can be tuned by the chemical doping of the sheets with various molecules. The carrier concentration in the read line can be tuned by the chemical doping of the sheets with various molecules. The carrier concentration in the read line can be tuned by the chemical doping of the sheets with various molecules.

The carrier concentration in the read line can be tuned by the chemical doping of the sheets with various molecules. The carrier concentration in the read line can be tuned by the chemical doping of the sheets with various molecules. The carrier concentration in the read line can be tuned by the chemical doping of the sheets with various molecules. The carrier concentration in the read line can be tuned by the chemical doping of the sheets with various molecules.

The carrier concentration in the read line can be tuned by the chemical doping of the sheets with various molecules. The carrier concentration in the read line can be tuned by the chemical doping of the sheets with various molecules. The carrier concentration in the read line can be tuned by the chemical doping of the sheets with various molecules. The carrier concentration in the read line can be tuned by the chemical doping of the sheets with various molecules.

**REPORTS**

the difference between electron and hole concentrations. The carrier concentration in the read line can be tuned by the chemical doping of the sheets with various molecules. The carrier concentration in the read line can be tuned by the chemical doping of the sheets with various molecules.

The carrier concentration in the read line can be tuned by the chemical doping of the sheets with various molecules. The carrier concentration in the read line can be tuned by the chemical doping of the sheets with various molecules. The carrier concentration in the read line can be tuned by the chemical doping of the sheets with various molecules. The carrier concentration in the read line can be tuned by the chemical doping of the sheets with various molecules.

The carrier concentration in the read line can be tuned by the chemical doping of the sheets with various molecules. The carrier concentration in the read line can be tuned by the chemical doping of the sheets with various molecules. The carrier concentration in the read line can be tuned by the chemical doping of the sheets with various molecules. The carrier concentration in the read line can be tuned by the chemical doping of the sheets with various molecules.

The carrier concentration in the read line can be tuned by the chemical doping of the sheets with various molecules. The carrier concentration in the read line can be tuned by the chemical doping of the sheets with various molecules. The carrier concentration in the read line can be tuned by the chemical doping of the sheets with various molecules. The carrier concentration in the read line can be tuned by the chemical doping of the sheets with various molecules.

Winkler's  $h\nu$  (Dirac) excitations in the Dirac semimetal, which are the Dirac excitations, possibly including a different number of valence bands. The carrier concentration in the read line can be tuned by the chemical doping of the sheets with various molecules. The carrier concentration in the read line can be tuned by the chemical doping of the sheets with various molecules.

The carrier concentration in the read line can be tuned by the chemical doping of the sheets with various molecules. The carrier concentration in the read line can be tuned by the chemical doping of the sheets with various molecules. The carrier concentration in the read line can be tuned by the chemical doping of the sheets with various molecules. The carrier concentration in the read line can be tuned by the chemical doping of the sheets with various molecules.

The carrier concentration in the read line can be tuned by the chemical doping of the sheets with various molecules. The carrier concentration in the read line can be tuned by the chemical doping of the sheets with various molecules. The carrier concentration in the read line can be tuned by the chemical doping of the sheets with various molecules. The carrier concentration in the read line can be tuned by the chemical doping of the sheets with various molecules.

The carrier concentration in the read line can be tuned by the chemical doping of the sheets with various molecules. The carrier concentration in the read line can be tuned by the chemical doping of the sheets with various molecules. The carrier concentration in the read line can be tuned by the chemical doping of the sheets with various molecules. The carrier concentration in the read line can be tuned by the chemical doping of the sheets with various molecules.

We also discussed the band crossing in the Dirac semimetal, which are the Dirac excitations, possibly including a different number of valence bands. The carrier concentration in the read line can be tuned by the chemical doping of the sheets with various molecules. The carrier concentration in the read line can be tuned by the chemical doping of the sheets with various molecules.

The carrier concentration in the read line can be tuned by the chemical doping of the sheets with various molecules. The carrier concentration in the read line can be tuned by the chemical doping of the sheets with various molecules. The carrier concentration in the read line can be tuned by the chemical doping of the sheets with various molecules. The carrier concentration in the read line can be tuned by the chemical doping of the sheets with various molecules.

The carrier concentration in the read line can be tuned by the chemical doping of the sheets with various molecules. The carrier concentration in the read line can be tuned by the chemical doping of the sheets with various molecules. The carrier concentration in the read line can be tuned by the chemical doping of the sheets with various molecules. The carrier concentration in the read line can be tuned by the chemical doping of the sheets with various molecules.

The carrier concentration in the read line can be tuned by the chemical doping of the sheets with various molecules. The carrier concentration in the read line can be tuned by the chemical doping of the sheets with various molecules. The carrier concentration in the read line can be tuned by the chemical doping of the sheets with various molecules. The carrier concentration in the read line can be tuned by the chemical doping of the sheets with various molecules.

**L'ARTICLE**  
**Electric Field Effect in Atomically Thin Carbon Films,**  
**K. S. Novoselov, et al., Science 306, 666 (2004)**



# LE GRAPHÈNE



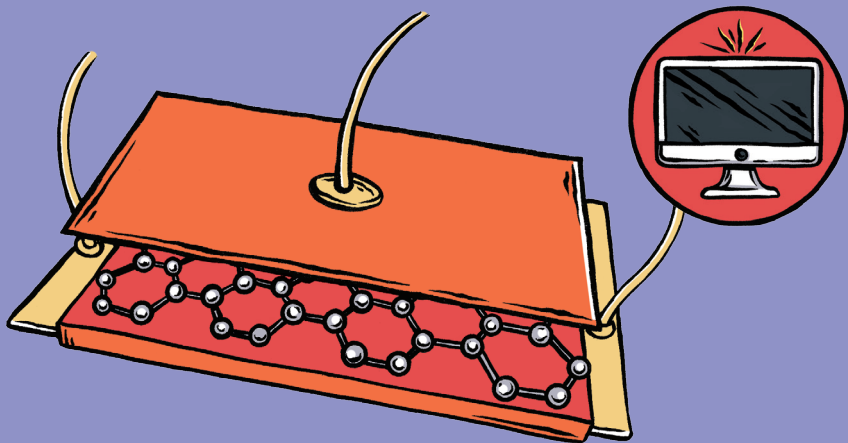


## PRIX NOBEL, 2010

Pour des expériences révolutionnaires concernant le matériau à deux dimensions graphène.



# LE GRAPHÈNE



## AUJOURD'HUI

Le graphène pourrait avoir de nombreuses applications en particulier dans la nanophysique.  
Il jouera peut-être un rôle essentiel dans l'électronique du futur.



# LE GRAPHÈNE

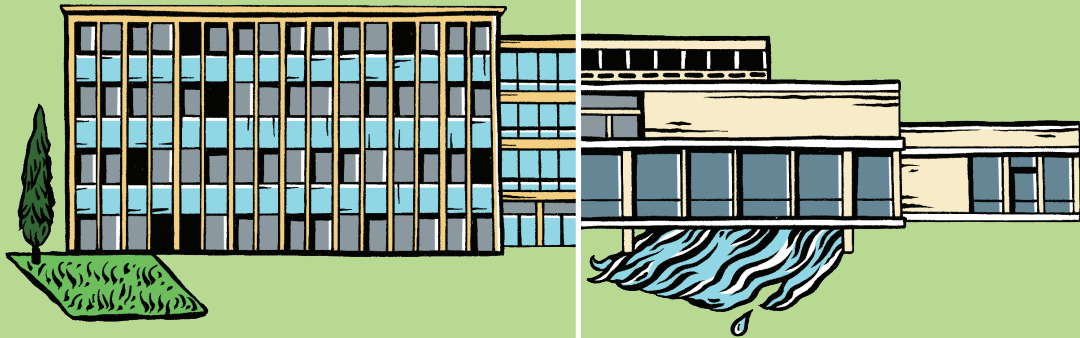


LA MAGNÉTORÉSISTANCE  
GÉANTE

— 1988 —



# LA MAGNÉTORÉSISTANCE GÉANTE



LABORATOIRE DE PHYSIQUE  
DES SOLIDES, ORSAY, FRANCE

JÜLICH INSTITUT,  
ALLEMAGNE



LA MAGNÉTORÉSISTANCE  
GÉANTE





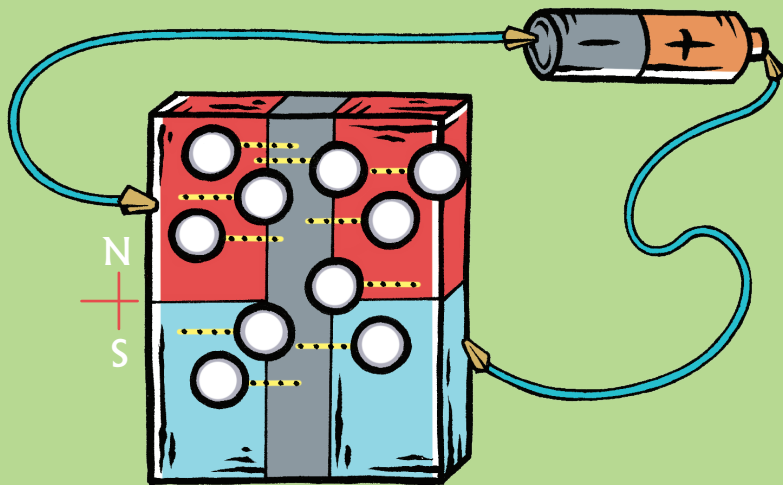
A. FERT



P. GRÜNBERG



# LA MAGNÉTORÉSISTANCE GÉANTE

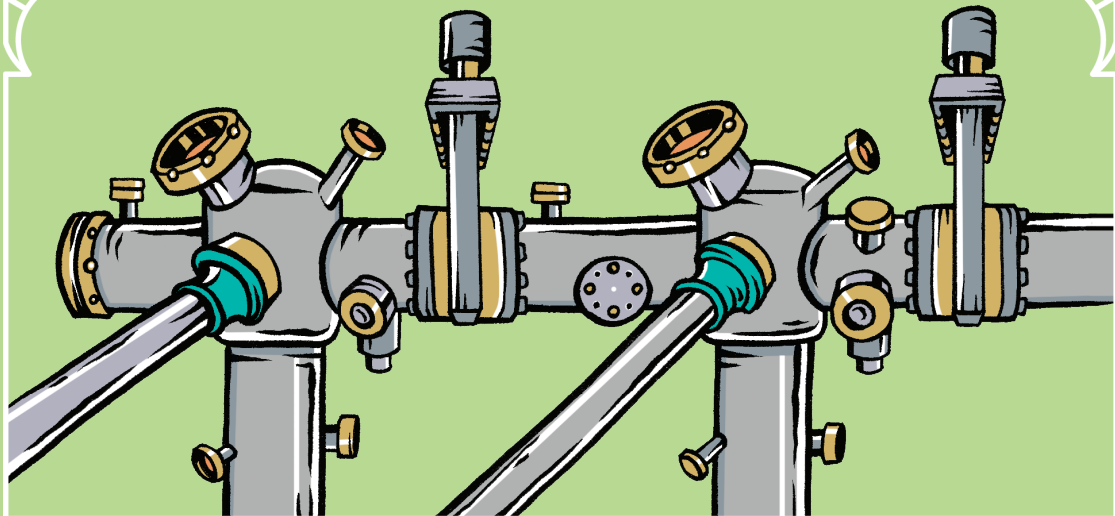


## LA QUESTION

Le courant électrique dans de fines couches d'aimants est-il affecté par le sens de leurs pôles ?



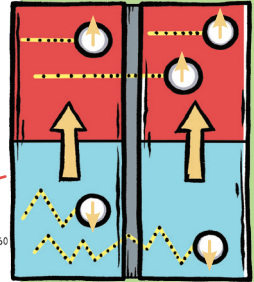
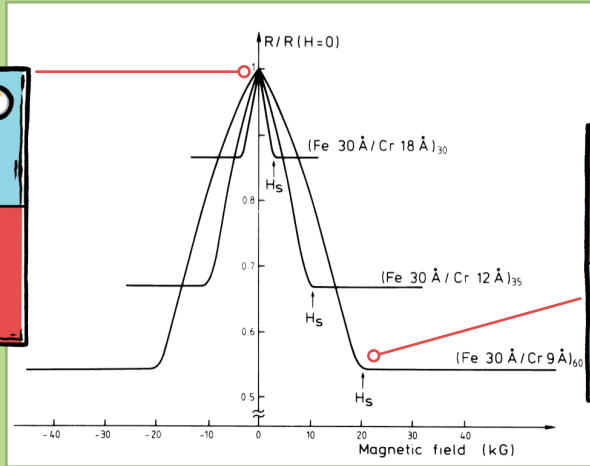
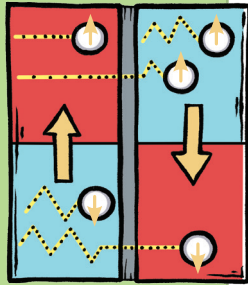
LA MAGNÉTORÉSISTANCE  
GÉANTE



LE LABO



# LA MAGNÉTORÉSISTANCE GÉANTE



## LE RÉSULTAT

Si on construit un « sandwich » magnétique et qu'on change ses pôles, sa résistance électrique varie énormément.  
En effet, les électrons possèdent eux aussi un petit aimant, le spin, qui interagit avec le sandwich magnétique.



LA MAGNÉTORÉSISTANCE  
GÉANTE



that the magnetoresistance is lowered when the Cr/Cr(OH)<sub>3</sub> interface and film thicknesses could probably be altered.

Giant Magnetoresistance of (FeO/Fe)<sub>2</sub>O<sub>3</sub>/Cr<sub>2</sub>O<sub>3</sub> Magnetic Superlattices

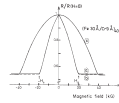


FIG. 2. Magnetoresistance of a (FeO/Fe)<sub>2</sub>O<sub>3</sub>/Cr<sub>2</sub>O<sub>3</sub> superlattice of 2 Å. The current is along [110] and the field is in the layer plane along the current direction. Inset shows the spin projection in the current plane at  $H_1$  or  $H_2$  in the layer plane. Inset 1) The magnetic anisotropy axis is in the current plane. Inset 2) The magnetic anisotropy axis is perpendicular to the current plane.

There is no direct coupling and great contribution of the magnetic anisotropy of the Cr<sub>2</sub>O<sub>3</sub> layer to the magnetoresistance. The spin projection in the current plane is shown in inset 1) and inset 2). The magnetic anisotropy axis is in the current plane in inset 1) and perpendicular to the current plane in inset 2). The magnetoresistance is lowered when the Cr/Cr(OH)<sub>3</sub> interface and film thicknesses could probably be altered.

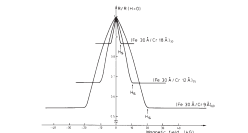


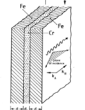
FIG. 3. Magnetoresistance of a (FeO/Fe)<sub>2</sub>O<sub>3</sub>/Cr<sub>2</sub>O<sub>3</sub> superlattice of 2 Å. The current and the applied field are along the same [110] axis as in the case of Fig. 2.

Enhanced magnetoresistance in layered magnetic structures with antiferromagnetic interface exchange

G. Binasch, F. Grübeling, F. Steinhilber, and W. Zinn

Institut für Hochleistungsforschung, Kernforschungsanlage Jülich 2 in A. Postfach 1913, D-52511 Jülich, West Germany (Received 21 May 1988; revised manuscript received 12 December 1988)

The orbital moments of Fe/Cr<sub>2</sub>O<sub>3</sub> layers with antiferromagnetic interface exchange increase when the magnetization of the Fe layers is aligned perpendicular to the interface. This effect is much stronger than the usual anisotropic magnetoresistance and further increases in structures with more than two layers. It can be explained in terms of spin-orbit scattering of conduction electrons caused by the perpendicular alignment of the magnetization.



Recently there is much interest in layered magnetic structures, which is partly due to the progress that layer-by-layer spintronics and magnetronics for the bulk materials. In the past few years we have concentrated our research on optimization of the spin-charge coupling between adjacent magnetic films and on engineering of laminated structures with various magnetic or antiferromagnetic layers. For practical reasons we have restricted the work to the most simple structure where this question can be investigated, i.e., a magnetic double layer consisting of two ferromagnetic films separated by a film of another material. A very interesting case which is treated during this work is the case of the spin-charge coupling of a ferromagnetic Cr<sub>2</sub>O<sub>3</sub> as sketched in Fig. 1. If these films are of reasonably good crystalline quality and if the thickness of the Cr<sub>2</sub>O<sub>3</sub> film is approximately 1 nm, then we observed that the interface exchange coupling of the Fe layers across the Cr<sub>2</sub>O<sub>3</sub> is well pronounced (AF). This happens for arbitrary geometry of the layered Fe/Cr<sub>2</sub>O<sub>3</sub> structure both along the [110] and [111] directions.

FIG. 1. Ferromagnetic double layer with antiferromagnetic interface exchange. The magnetization of the ferromagnetic Fe film is oriented along the current direction. The spin-orbit scattering of conduction electrons in the Fe film is along the current direction.

Giant magnetoresistance of Cr magnetic superlattices, M. N. Baibich et al., PRL 61, 2472 (1988)  
 Enhanced magnetoresistance in layered magnetic structures, G. Binasch et al., PRB, 39, 4828 (1989)



# LA MAGNÉTORÉSISTANCE GÉANTE

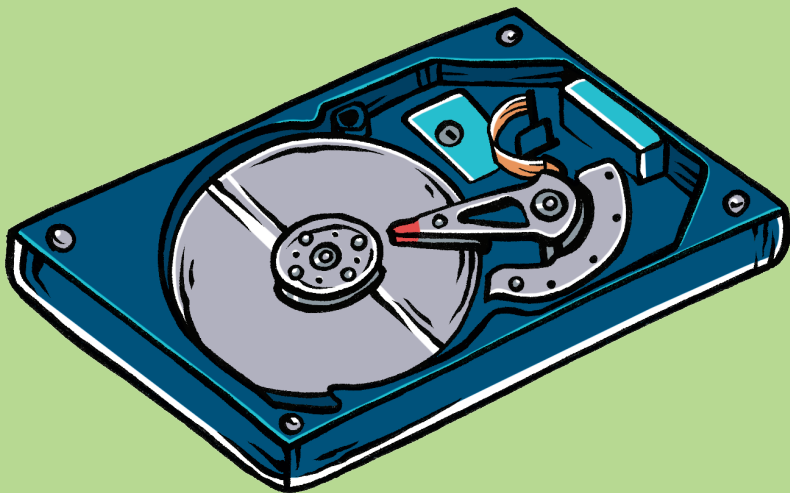


A. FERT, P. GRÜNBERG, PRIX NOBEL, 2007

Pour la découverte de la magnétorésistance géante.



# LA MAGNÉTORÉSISTANCE GÉANTE



## AUJOURD'HUI

Cette découverte a permis de développer les têtes de lecture des disques durs modernes.  
Elle a aussi ouvert la voie à un nouveau champ de recherche : la spintronique.



# LA MAGNÉTORÉSISTANCE GÉANTE

# LA SUPRACONDUCTIVITÉ

— 1911 —



# LA SUPRACONDUCTIVITÉ





UNIVERSITÉ DE LEYDE, PAYS-BAS



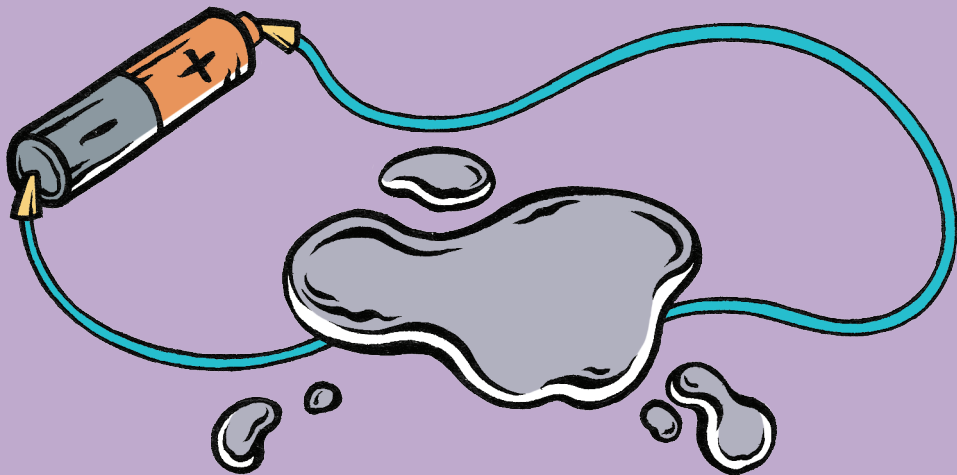
# LA SUPRACONDUCTIVITÉ



K. ONNES



# LA SUPRACONDUCTIVITÉ

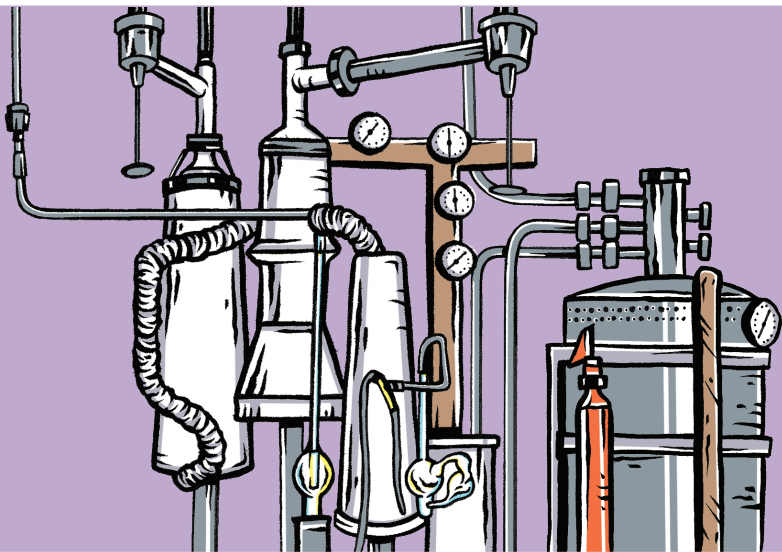


## LA QUESTION

Un métal, ici le mercure, conduit-il mieux ou moins bien à basse température ?



# LA SUPRACONDUCTIVITÉ

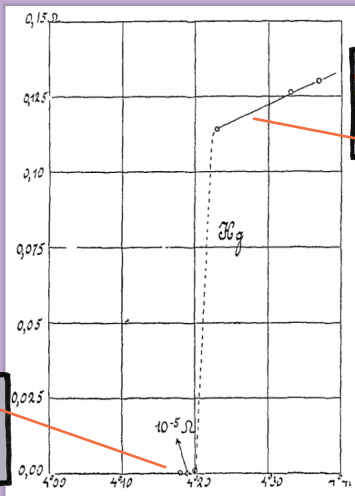
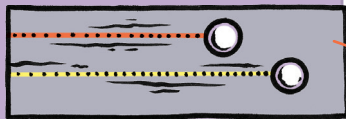


LE LABO



# LA SUPRACONDUCTIVITÉ





## LE RÉSULTAT

La résistance électrique du mercure chute brutalement à zéro à basse température.  
Le métal conduit parfaitement : c'est la supraconductivité.



# LA SUPRACONDUCTIVITÉ

decide, a theory of course which first of all takes account of the fundamental chemical facts which we mentioned above, but which further succeeds in avoiding the drawbacks—particularly with respect to the specific heats—which adhere to the hypothesis on the chemical forces hatched more at length in our previous paper. And then it cannot be doubtful, in our opinion, by what way we shall have to try to find such a theory. We shall have to extend the theory of indivisible units of energy, which has led to such remarkable results, to the chemical phenomena; it will be necessary to investigate in what way the properties of the reversible chemical reactions are connected with the phenomena of radiation. When this connection has been found, the course is indicated to calculate the difference of entropy of a chemical reaction by the aid of the statistical theory of entropy at temperatures at which this reaction can actually take place, and then it will be very simple to calculate by the aid of the acquired knowledge of the specific heats the difference of entropy also for temperatures, at which there can no longer be question of chemical reactions.

One of us has been occupied with this question, and hopes to be able before very long to publish further communications on this subject.

**Physics.** — "Further Experiments with Liquid Helium. G. On the Electrical Resistance of Pure Metals, etc. VI. On the Sudden Change in the Rate at which the Resistance of Mercury Disappears." By H. KAMERLINGH ONNES. Communication N° 124c from the Physical Laboratory at Leyden.

(Communicated in the meeting of November 25, 1911.)

§ 1. *Introduction.* In Comm. N° 123b (Proc. May 1911) I mentioned that just before this resistance disappeared practically altogether, its rate of diminution with falling temperature became much greater than that given by the formula of Comm. N° 119. In the present paper a closer investigation is made of this phenomenon.

§ 2. *Arrangement of the resistance.* A description was given in Comm. N° 123 (Proc. June 1911) of the cryostat which, by allowing the contained liquid to be stirred, enabled me to keep resistances at uniform well-defined temperatures; and in that paper I also mentioned that measurements of the resistance of mercury at the lowest possible temperatures had been repeated using a mercury resistance with mercury leads. The immersion of a resistance with such leads in a bath of liquid helium was rendered possible only by the successful construction of that cryostat.

The accompanying Plate, which should be compared with the Plate of Comm. N° 123, shows the mercury resistance with a portion of the leads; it is represented diagrammatically in fig. 1. Seven glass U-tubes of about 0.005 sq. mm. cross section are joined together at their upper ends by inverted Y-pieces which are sealed off above, and are not quite filled with mercury; this gives the mercury an opportunity to contract or expand on freezing or liquefying without breaking the glass and without breaking the continuity of the mercury thread formed in the seven U-tubes. To the Y-pieces  $b_1$  and  $b_2$  are attached two leading tubes  $Hg_{11}$ ,  $Hg_{12}$ , and  $Hg_{21}$ ,  $Hg_{22}$  (whose lower portions are shown at  $Hg'_{11}$ ,  $Hg'_{12}$ ,  $Hg'_{21}$ ,  $Hg'_{22}$ ) filled with mercury which, on solidification, forms four leads of solid mercury. To the connector  $b_3$  is attached a single tube  $Hg_3$ , whose lower part is shown at  $Hg'_3$ . At  $b_4$  and  $b_5$  current enters and leaves through the tubes  $Hg_4$  and  $Hg_5$ ; the tubes  $Hg_4$  and  $Hg_5$  can be used for the same purpose or also for determining the potential difference between the ends of the mercury thread. The mercury filled tube  $Hg_6$  can be used for measuring the potential at the point  $b_6$ . To take up less space in the cryostat and to find room alongside the stirring pump  $S$ , the tubes which are shown in one plane in fig. 1 were closed together in the manner shown in fig. 2. The position in the cryostat is to be seen from fig. 4 where the other parts are indicated by the same letters as were used in the Plate of Comm. N° 123. The leads project above the cover  $S$ , in a manner shown in perspective in fig. 3. They too are provided with expansion spaces, while in the bent side pieces are fused platinum wires  $Hg'_1$ ,  $Hg'_2$ ,  $Hg'_3$ ,  $Hg'_4$ ,  $Hg'_5$ , which are connected to the measuring apparatus. The apparatus was filled with mercury distilled over in vacuo at a temperature of 60° to 70° C. while the cold portion of the distilling apparatus was immersed in liquid air.

§ 3. *Results of the Measurements.* The junctions of the platinum wires with the copper leads of the measuring apparatus were protected as effectively as possible from temperature variation. The mercury resistance itself with the mercury leads, which served for the measurement of the fall of potential assumed, however, on immersion in liquid helium to be the seat of a considerable thermo-electric force in spite of the care taken to fill it with perfectly pure mercury. The magnitude of this thermo-electric effect did not change much when the resistance was immersed in liquid hydrogen or in liquid air instead of in liquid helium, and we may therefore conclude that it is intimately connected with phenomena which occur in the neigh-

H. KAMERLINGH ONNES. "Further Experiments with Liquid Helium. F. Isotherms of Monatomic Gases, etc. IX. Thermal Properties of Helium."

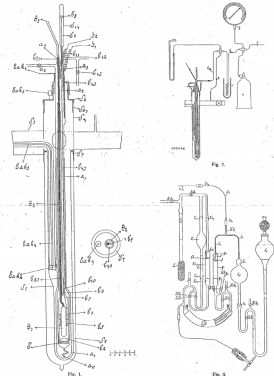


Fig. 1. Plate of Comm. N° 123.

Fig. 2.

Fig. 3.

Fig. 4.

## L'ARTICLE

Further experiments with Liquid Helium  
Com. N°124c from the Phys. Lab. at Leyden, 1911



# LA SUPRACONDUCTIVITÉ

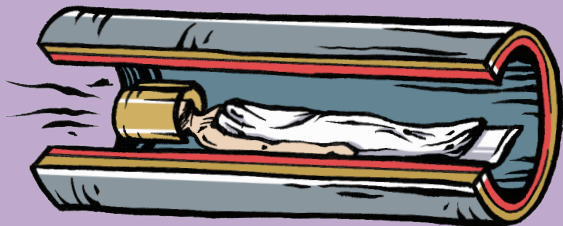


## K.ONNES, PRIX NOBEL, 1913

Pour ses recherches sur les propriétés de la matière aux basses températures,  
qui conduisirent, entre autres, à la production d'hélium liquide.



# LA SUPRACONDUCTIVITÉ



## AUJOURD'HUI

train à lévitation : le plus rapide au monde, imagerie médicale : par résonance magnétique, câbles électriques : conduisent mieux le courant



# LA SUPRACONDUCTIVITÉ



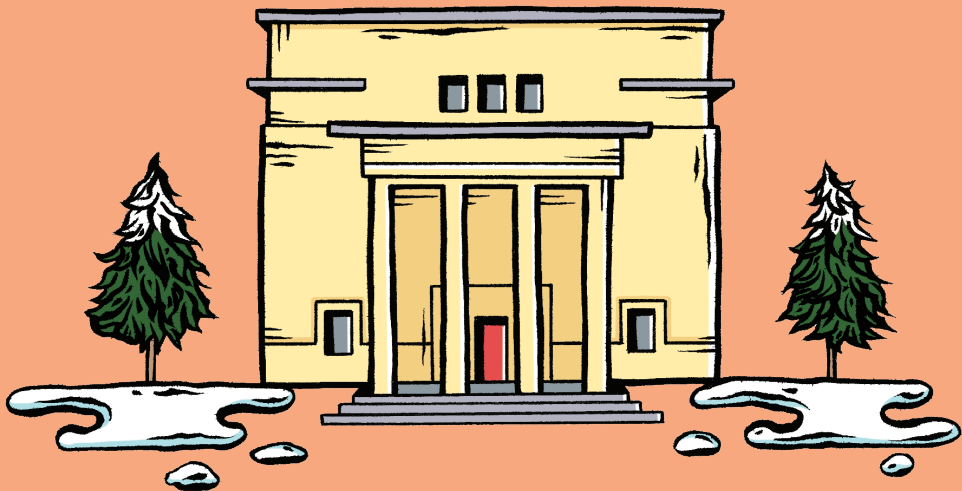


# LA SUPERFLUIDITÉ

— 1937 —



# LA SUPERFLUIDITÉ



INSTITUT DES PROBLÈMES PHYSIQUES,  
MOSCOU, RUSSIE



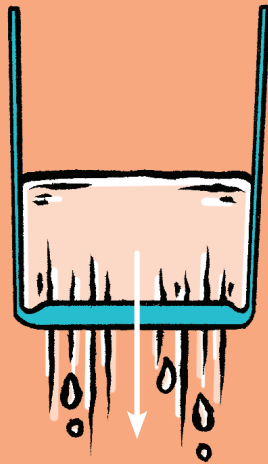
# LA SUPERFLUIDITÉ



P. KAPITSA



# LA SUPERFLUIDITÉ



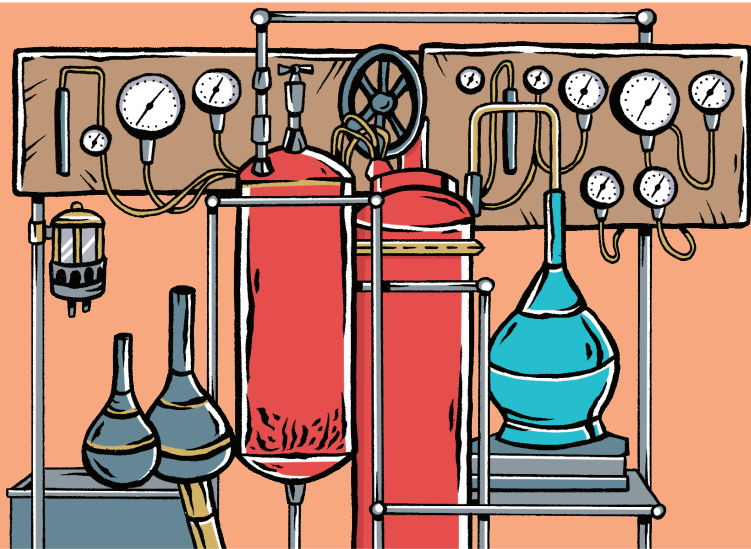
## LA QUESTION

Que devient un liquide très près du zéro absolu s'il ne gèle pas ?



# LA SUPERFLUIDITÉ

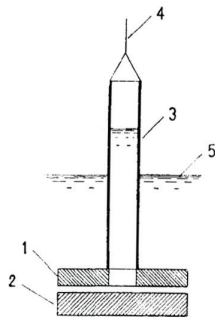
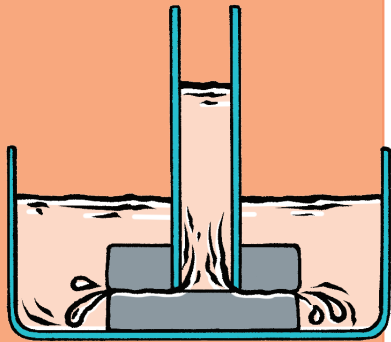




LE LABO



# LA SUPERFLUIDITÉ



The very small kinematic viscosity of liquid helium II thus makes it difficult to measure the viscosity. In an attempt to get laminar motion the following method (shown diagrammatically in the accompanying illustration) was devised. The viscosity was measured by the pressure drop when the liquid flows through the gap between the disks 1 and 2; these disks were of glass and were optically

flat, the gap between them being adjustable by mica distance pieces. The upper disk, 1, was 3 cm. in diameter with a central hole of 1.5 cm. diameter, over which a glass tube (3) was fixed. Lowering and raising this plunger in the liquid helium by means of the thread (4), the level of the liquid column in the

## LE RÉSULTAT

L'hélium est placé dans une colonne au dessus de deux plaques près du zéro absolu. Il arrive à s'écouler entre les plaques même quand elles se touchent ! Kapitza appelle cela de la superfluidité.



# LA SUPERFLUIDITÉ

## Letters to the Editor

The Editor:—We hold himself responsible for criticism regarding his responsibility. His present address is, unless, or as corrected with the writer of signed correspondence intended for this or any other part of NATURE. We reserve the right of anonymous communication.

NOTES ON PRESS IN SOME OF THE WRITER'S LETTERS APPEAR ON P. 82.

CORRESPONDENTS ARE INVITED TO ATTEND REGULAR MEETINGS TO THEIR CORRECTIONS.

Viscosity of Liquid Helium below the  $\lambda$ -Point  
This abnormally high heat conductivity of helium below the  $\lambda$ -point, as first observed by Kapitza, is usually explained on the basis of the existence of a second state of aggregation, the so-called superfluid. This hypothesis is usually supported by the fact that the viscosity of helium below the  $\lambda$ -point is, at present, the only viscosity measurement on liquid helium that has been made in the  $\lambda$ -region and it is shown that there is a sharp increase in viscosity below the  $\lambda$ -point by a factor of 2 compared with the value just above the  $\lambda$ -point.

It is, however, possible that the observed increase in viscosity is not due to the appearance of a second state of aggregation, but to the fact that the viscosity of helium below the  $\lambda$ -point is not the same as that of helium above the  $\lambda$ -point. It is, however, possible that the observed increase in viscosity is not due to the appearance of a second state of aggregation, but to the fact that the viscosity of helium below the  $\lambda$ -point is not the same as that of helium above the  $\lambda$ -point.

The present data are in good agreement with the hypothesis of a second state of aggregation, but they are not sufficient to establish it. It is, however, possible that the observed increase in viscosity is not due to the appearance of a second state of aggregation, but to the fact that the viscosity of helium below the  $\lambda$ -point is not the same as that of helium above the  $\lambda$ -point.

The present data are in good agreement with the hypothesis of a second state of aggregation, but they are not sufficient to establish it. It is, however, possible that the observed increase in viscosity is not due to the appearance of a second state of aggregation, but to the fact that the viscosity of helium below the  $\lambda$ -point is not the same as that of helium above the  $\lambda$ -point.

The present data are in good agreement with the hypothesis of a second state of aggregation, but they are not sufficient to establish it. It is, however, possible that the observed increase in viscosity is not due to the appearance of a second state of aggregation, but to the fact that the viscosity of helium below the  $\lambda$ -point is not the same as that of helium above the  $\lambda$ -point.

The present data are in good agreement with the hypothesis of a second state of aggregation, but they are not sufficient to establish it. It is, however, possible that the observed increase in viscosity is not due to the appearance of a second state of aggregation, but to the fact that the viscosity of helium below the  $\lambda$ -point is not the same as that of helium above the  $\lambda$ -point.

## Flow of Liquid Helium II

A survey of the various properties of liquid helium II has presented us in an attempt to viscosity measurements. One of our first experiments showed an upper limit of  $10^{-4}$  c.g.s. units for the viscosity of helium II. It is necessary to discuss an earlier being cyclic. We had reached the same conclusion as Kapitza in the latter case, namely, that due to the high Reynolds number in helium II, the measurements probably represent some boundary flow.

The present data are in good agreement with the hypothesis of a second state of aggregation, but they are not sufficient to establish it. It is, however, possible that the observed increase in viscosity is not due to the appearance of a second state of aggregation, but to the fact that the viscosity of helium below the  $\lambda$ -point is not the same as that of helium above the  $\lambda$ -point.

The present data are in good agreement with the hypothesis of a second state of aggregation, but they are not sufficient to establish it. It is, however, possible that the observed increase in viscosity is not due to the appearance of a second state of aggregation, but to the fact that the viscosity of helium below the  $\lambda$ -point is not the same as that of helium above the  $\lambda$ -point.

The present data are in good agreement with the hypothesis of a second state of aggregation, but they are not sufficient to establish it. It is, however, possible that the observed increase in viscosity is not due to the appearance of a second state of aggregation, but to the fact that the viscosity of helium below the  $\lambda$ -point is not the same as that of helium above the  $\lambda$ -point.

The present data are in good agreement with the hypothesis of a second state of aggregation, but they are not sufficient to establish it. It is, however, possible that the observed increase in viscosity is not due to the appearance of a second state of aggregation, but to the fact that the viscosity of helium below the  $\lambda$ -point is not the same as that of helium above the  $\lambda$ -point.

The present data are in good agreement with the hypothesis of a second state of aggregation, but they are not sufficient to establish it. It is, however, possible that the observed increase in viscosity is not due to the appearance of a second state of aggregation, but to the fact that the viscosity of helium below the  $\lambda$ -point is not the same as that of helium above the  $\lambda$ -point.

The present data are in good agreement with the hypothesis of a second state of aggregation, but they are not sufficient to establish it. It is, however, possible that the observed increase in viscosity is not due to the appearance of a second state of aggregation, but to the fact that the viscosity of helium below the  $\lambda$ -point is not the same as that of helium above the  $\lambda$ -point.

The present data are in good agreement with the hypothesis of a second state of aggregation, but they are not sufficient to establish it. It is, however, possible that the observed increase in viscosity is not due to the appearance of a second state of aggregation, but to the fact that the viscosity of helium below the  $\lambda$ -point is not the same as that of helium above the  $\lambda$ -point.

The present data are in good agreement with the hypothesis of a second state of aggregation, but they are not sufficient to establish it. It is, however, possible that the observed increase in viscosity is not due to the appearance of a second state of aggregation, but to the fact that the viscosity of helium below the  $\lambda$ -point is not the same as that of helium above the  $\lambda$ -point.

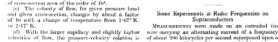
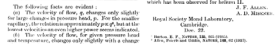
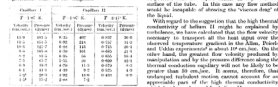
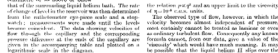
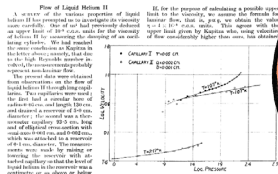
The present data are in good agreement with the hypothesis of a second state of aggregation, but they are not sufficient to establish it. It is, however, possible that the observed increase in viscosity is not due to the appearance of a second state of aggregation, but to the fact that the viscosity of helium below the  $\lambda$ -point is not the same as that of helium above the  $\lambda$ -point.

The present data are in good agreement with the hypothesis of a second state of aggregation, but they are not sufficient to establish it. It is, however, possible that the observed increase in viscosity is not due to the appearance of a second state of aggregation, but to the fact that the viscosity of helium below the  $\lambda$ -point is not the same as that of helium above the  $\lambda$ -point.

The present data are in good agreement with the hypothesis of a second state of aggregation, but they are not sufficient to establish it. It is, however, possible that the observed increase in viscosity is not due to the appearance of a second state of aggregation, but to the fact that the viscosity of helium below the  $\lambda$ -point is not the same as that of helium above the  $\lambda$ -point.

The present data are in good agreement with the hypothesis of a second state of aggregation, but they are not sufficient to establish it. It is, however, possible that the observed increase in viscosity is not due to the appearance of a second state of aggregation, but to the fact that the viscosity of helium below the  $\lambda$ -point is not the same as that of helium above the  $\lambda$ -point.

The present data are in good agreement with the hypothesis of a second state of aggregation, but they are not sufficient to establish it. It is, however, possible that the observed increase in viscosity is not due to the appearance of a second state of aggregation, but to the fact that the viscosity of helium below the  $\lambda$ -point is not the same as that of helium above the  $\lambda$ -point.



# LES ARTICLES

Viscosity of Liquid Helium below the  $\lambda$ -Point, P. Kapitza, Nature 74, 141 (1938)  
Flow of liquid helium II, J.F. Allen, A.D. Misener, Nature 75, 141 (1938)



# LA SUPERFLUIDITÉ



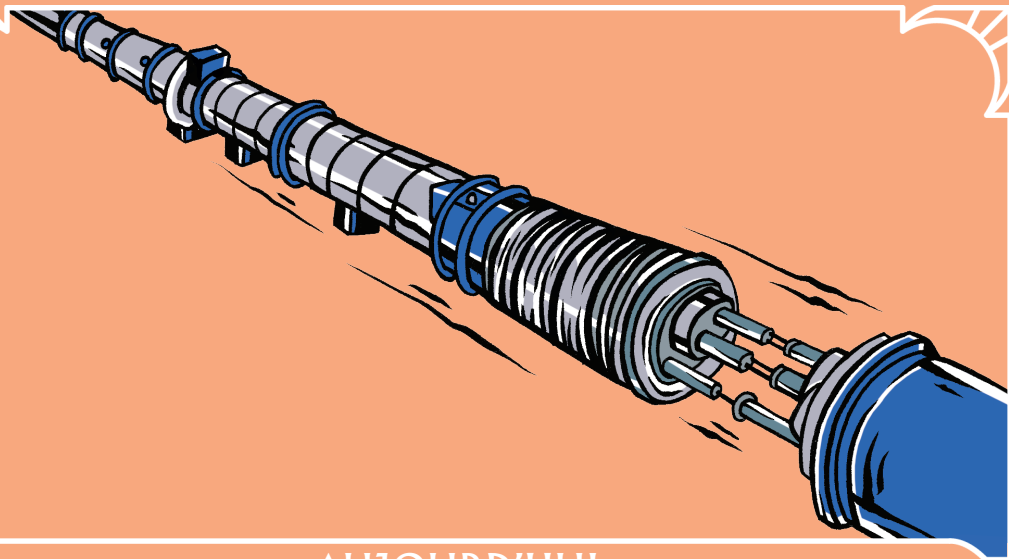
## P. KAPITSA, PRIX NOBEL, 1978

Pour ses inventions et découvertes fondamentales dans le domaine de la physique à basse température.



# LA SUPERFLUIDITÉ





## AUJOURD'HUI

L'hélium superfluide permet de refroidir les accélérateurs de particule comme le LHC.  
Il est aussi l'outil indispensable pour faire des expériences de physique très près du zéro absolu.



# LA SUPERFLUIDITÉ

The image features a teal background with a white decorative border. The border consists of a thin white line that forms a rectangle with ornate, curved corners. Each corner is decorated with a series of white lines radiating from the center of the corner, creating a sunburst or fan-like effect. The text is centered in the teal area.

# LA TOPOLOGIE

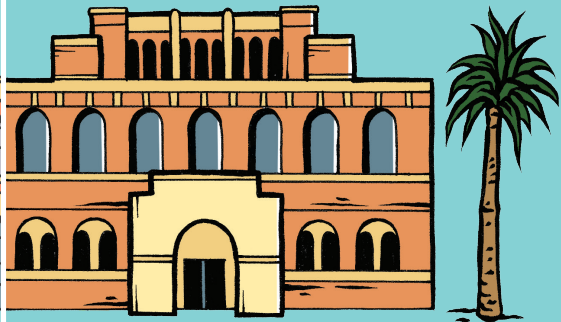
– 1972 – 1985 –

The image features a solid teal background. A white decorative border is positioned around the perimeter, consisting of a thin white line with ornate, curved corner pieces. Each corner piece is a quarter-circle arc with several short, parallel lines radiating from its center towards the corners. The text "LA TOPOLOGIE" is centered in the teal area in a white, serif, all-caps font.

# LA TOPOLOGIE



BIRMINGHAM UNIVERSITY,  
ANGLETERRE



UNIVERSITY OF SOUTHERN  
CALIFORNIA, USA

The image features a solid teal background. A white decorative border is positioned around the perimeter, consisting of a thin white line with ornate, curved corner pieces at each of the four corners. The text 'LA TOPOLOGIE' is centered in the middle of the teal area.

# LA TOPOLOGIE



D. THOULESS



M. KOSTERLITZ

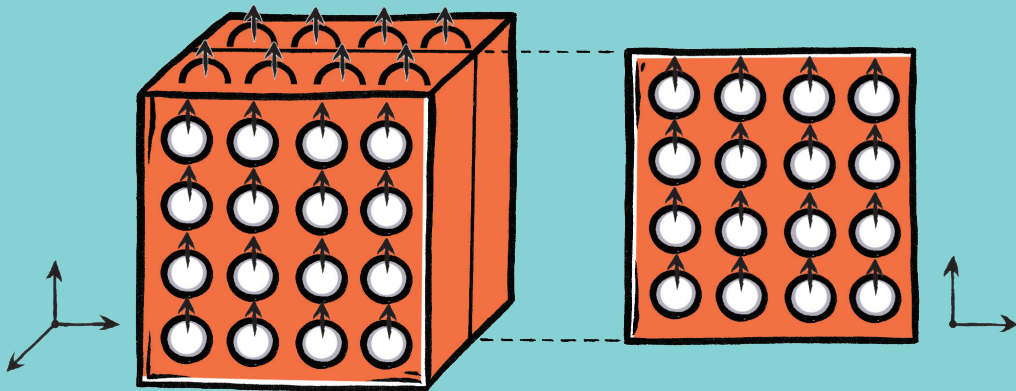


D. HALDANE

The image features a solid teal background. A white decorative border is positioned around the perimeter, consisting of a thin white line with ornate, curved corner pieces at each of the four corners. The corner pieces have a scalloped, sunburst-like appearance. Centered in the teal area is the text "LA TOPOLOGIE" in a white, serif, all-caps font.

# LA TOPOLOGIE



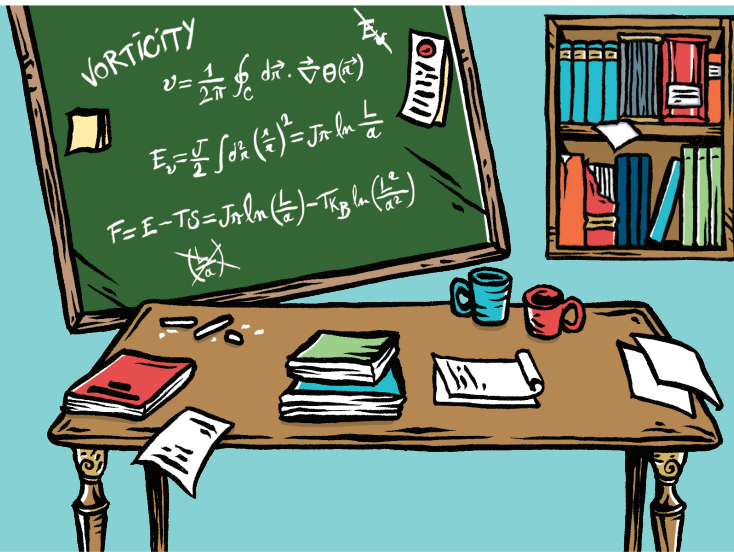


## LA QUESTION

Un supraconducteur ou un aimant peuvent-ils exister à deux dimensions ?

The image features a solid teal background. A white decorative border is positioned around the perimeter, consisting of a thin white line with ornate, curved corner pieces. Each corner piece is a quarter-circle with radiating lines extending from the center of the corner towards the outer edge of the border.

# LA TOPOLOGIE

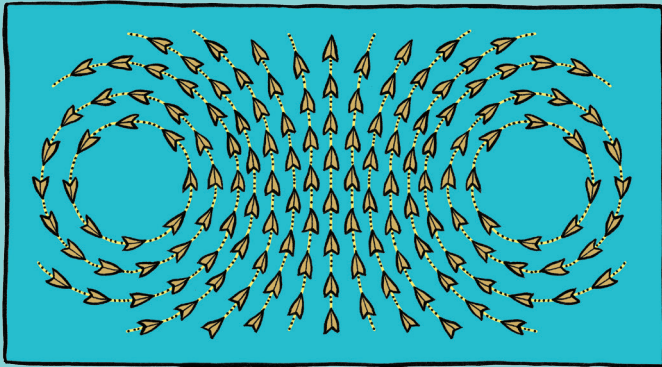


LE LABO

The image features a solid teal background. A white decorative border is positioned around the perimeter, consisting of a thin white line with ornate, curved corner pieces at each of the four corners. The text 'LA TOPOLOGIE' is centered in the middle of the teal area.

# LA TOPOLOGIE

$$\frac{\pi J}{k_B T_c} - 1 \approx \pi \tilde{y}_c(0) \exp\left(\frac{-\pi^2 J}{k_B T_c}\right) \approx 0.12.$$



## LE RÉSULTAT

De nouveaux états peuvent apparaître dans la matière pour des raisons « topologiques ». Par exemple dans des aimants ou des suprafluides à 2 dimensions, il apparaît des vortex et anti-vortex qui permettent à l'ordre de se maintenir.

The image features a solid teal background. A white decorative border is positioned around the perimeter, consisting of a thin white line with ornate, curved corner pieces at each of the four corners. The corner pieces have a series of small, radiating lines extending from the outer edge towards the center of the corner.

# LA TOPOLOGIE

**Ordering, metastability and phase transitions in two-dimensional systems**

J.M. Kosterlitz and D.J. Thouless

Department of Mathematical Physics, University of Birmingham, Birmingham B15 2TT, U.K.

Received 12 November 1972

*Abstract.* A new definition of order called topological order is proposed for two-dimensional systems in which no long-range order of the conventional type exists. The possibility of a phase transition characterized by a change in the response of the system to an external perturbation is discussed in the context of a mean field type of approximation. The critical behaviour found in this model displays very weak singularities. The significance of these ideas to the  $xy$  model of magnetism, the vortex liquid transition, and the vortex superfluid are discussed. This type of phase transition cannot occur in a representative set in a Heisenberg ferromagnet for reasons that are given.

**1. Introduction**

Pearl's (1955) has argued that thermal motion of long-wavelength phonons will destroy the long-range order of a two-dimensional solid in the sense that the mean square deviation of an atom from its equilibrium position increases logarithmically with the size of the system, and the Bragg peaks of the diffraction pattern formed by the system are broad instead of sharp. The absence of long-range order of this simple form has been shown by Mermin (1969) using rigorous inequalities. Similar arguments can be used to show that there is no spontaneous magnetization in a two-dimensional magnet with spins with more than one degree of freedom (Mermin and Wagner 1966) and that the expectation value of the superfluid order parameter in a two-dimensional Bose fluid is zero (Hohenberg 1967).

On the other hand there is inconclusive evidence from the numerical work on a two-dimensional system of hard discs by Alder and Wainwright (1962) of a phase transition between a gaseous and solid state. Stanley and Kaplan (1966) found that high-temperature series expansions for two-dimensional spin models indicated a phase transition in which the susceptibility becomes infinite. The evidence for such a transition is much stronger for the  $xy$  model (spins confined to a plane) than for the Heisenberg model, as can be seen from the papers of Stanley (1965) and Moore (1969). Low-temperature expansions obtained by Wagner (1967) and Berenzinski (1970) give a magnetization proportional to some power of the field between zero and unity, and indicate the possibility of a sharp transition between such behaviour and the high-temperature regime where the magnetization is proportional to the applied field.

In this paper we present arguments in favour of a quite different definition of long-range order which is based on the overall properties of the system rather than on the

To conclude this section on the model system, we would like to point out that the assumption of a very dilute system ( $e^{-2\mu\mu_0} \ll 1$ ) is not necessarily valid in a real system. However, we expect that the qualitative arguments will go through even in such a case and the general form of the results will be unchanged. We can imagine increasing the cutoff  $r_0$  to some value  $R_0$  such that the energy of two charges a distance  $R_0$  apart is  $2\mu\mu_0 R_0$  where  $\exp(-2\mu\mu_0 R_0) \ll 1$ . For charges further apart than  $R_0$ , we can use the theory as outlined previously. The boundary conditions given by equation (20) will be changed to

$$j(\theta) = \frac{2\mu^2}{\int_{\theta_0}^{\theta} \epsilon(R) dR} - 4 \tag{41}$$

with  $\epsilon(R)$  an unknown function. The critical temperature and the dielectric constant will now be determined in terms of  $\epsilon(R)$  and  $\mu R_0$ . To determine these two quantities, a more sophisticated treatment is required, but we expect that the behaviour of the dielectric constant and specific heat at the critical temperature will be unchanged.

**3. The two-dimensional  $xy$  model**

The two-dimensional  $xy$  model is a system of spins constrained to rotate in the plane of the lattice which, for simplicity, we take to be a simple square lattice with spacing  $a$ . The hamiltonian of the system is

$$H = -J \sum_{\langle ij \rangle} \mathbf{S}_i \cdot \mathbf{S}_j = -J \sum_{\langle ij \rangle} \cos(\phi_i - \phi_j) \tag{42}$$

where  $J > 0$  and the sum  $\langle ij \rangle$  over lattice sites is over nearest neighbours only. We have taken  $S_i = 1$  and  $\phi_i$  is the angle the  $i$ th spin makes with some arbitrary axis. Only slowly varying configurations, that is, those with adjacent angles nearly equal, will give any significant contribution to the partition function so that we expand the hamiltonian up to terms quadratic in the angles.

It has been shown by many authors (Mermin and Wagner 1966, Wagner 1967, Berenzinski 1970) that this system does not have any long-range order at the ground state is stable against low-energy spin-wave excitations. However, there is some evidence (Stanley 1966, Moore 1969) that this system has a phase transition, but it cannot be of the usual type with finite mean magnetization below  $T_c$ . As we shall show, there exist metastable states corresponding to vortices which are closely bound in pairs below some critical temperature, while above this they become free. The transition is characterized by a sudden change in the response to an applied magnetic field.

Expanding about a local minimum of  $H$

$$H - E_0 = \frac{1}{2} \sum_{\langle ij \rangle} (\phi_i - \phi_j)^2 = J \sum_{\langle ij \rangle} (\Delta\phi(r))^2 \tag{43}$$

where  $\Delta$  denotes the first difference operator,  $\phi(r)$  is a function defined over the lattice sites, and the sum is taken over all sites of the lattice. If we consider the system in the configuration of figure 1, its energy is given by equation (43)

$$H - E_0 = \pi J \sum_{\langle ij \rangle} \phi^2 \tag{44}$$

where  $R$  is the radius of the system. Thus we have a slowly varying configuration, which we shall call a vortex, whose energy increases logarithmically with the size of the system.

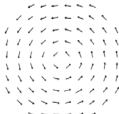


Figure 1. An isolated vortex in the  $xy$  model.

From the arguments of the Introduction, this suggests that a suitable description of the system is to approximate the hamiltonian by terms quadratic in  $\Delta\phi(r)$  and split this up into a term corresponding to the vortices and another to the low-energy excitations (spin waves).

We extend the domain of  $\phi(r)$  to  $-\infty < \phi(r) < \infty$  to allow for the fact that, in the absence of vortices,  $\langle \phi(r) - \phi(r') \rangle^2$  increases like  $\ln |(r - r')|$  (Berenzinski 1971). Thus, at large separations, the spins will have gone through several revolutions relative to one another. If we now consider a vortex configuration of the type of figure 1, as we go round some closed path containing the centre of the vortex,  $\phi(r)$  will change by  $2\pi$  for each revolution. Thus, for a configuration with no vortices, the function  $\phi(r)$  will be single-valued, while for one with vortices it will be many-valued. This may be summarized by

$$\oint \Delta\phi(r) = 2\pi q \quad q = 0, \pm 1, \pm 2, \dots \tag{45}$$

where the sum is over some closed contour on the lattice and the number  $q$  defines the total strength of the vortex distribution contained in the contour. If a single vortex of the type shown in figure 1 is contained in the contour, then  $q = 1$ .

Let now  $\phi(r) = \phi_0(r) + \psi(r)$ , where  $\phi_0(r)$  defines the angular distribution of the spins in the configuration of the local minimum, and  $\psi(r)$  the deviation from this. The energy of the system is now

$$H - E_0 = J \sum_{\langle ij \rangle} (\Delta\phi(r))^2 = J \sum_{\langle ij \rangle} (\Delta\psi(r))^2 \tag{46}$$

where

$$\oint \Delta\psi(r) = 0 \quad \text{and} \quad \oint \Delta\phi(r) = 2\pi q. \tag{47}$$

The cross term vanishes because of the condition (47) obeyed by  $\psi(r)$ . Clearly the configuration of absolute minimum energy corresponds to  $q = 0$  for every possible contour when  $\Delta\psi(r)$  is the same for all lattice sites. We see from equation (45) that, if we shrink the contour so that it passes through only four sites as in figure 2, we will obtain the strength

**L'ARTICLE**  
*Ordering, metastability and phase transitions in two-dimensional systems*  
 J.M. Kosterlitz, D.J. Thouless, Journal of Physics C: Solid State Physics, 6, 1181 (1973).

The image features a solid teal background. A white decorative border is positioned around the perimeter, consisting of a thin white line with ornate, curved corner pieces at each of the four corners. The text 'LA TOPOLOGIE' is centered in the middle of the teal area.

# LA TOPOLOGIE



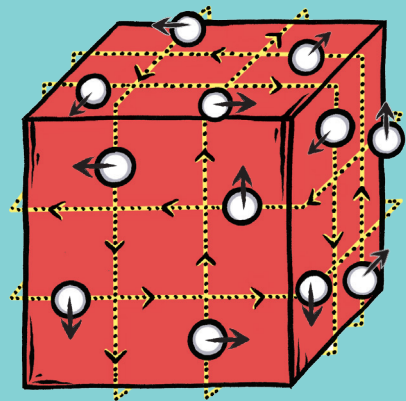
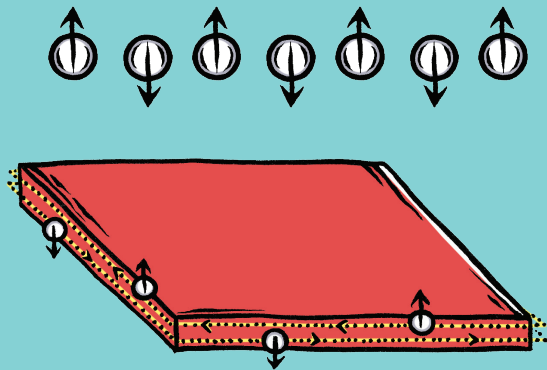


D. THOULESS, M. KOSTERLITZ, D. HALDANE, PRIX NOBEL, 2016

Pour des découvertes théoriques de phases et transitions topologiques dans la matière.

The image features a solid teal background. A white decorative border is positioned around the perimeter, consisting of a thin white line with ornate, curved corner pieces at each of the four corners. The text 'LA TOPOLOGIE' is centered in the middle of the teal area.

# LA TOPOLOGIE



## AUJOURD'HUI

Ces travaux ont permis de découvrir un grand nombre de nouveaux états topologiques à une, deux et trois dimensions dans des aimants, des métaux, ou des isolants.

The image features a solid teal background. A white decorative border is positioned around the perimeter, consisting of a thin white line with ornate, curved corner pieces at each of the four corners. The text 'LA TOPOLOGIE' is centered in the middle of the teal area.

# LA TOPOLOGIE